

A phenomenological model for surface deposition kinetics during plasma and sputter deposition of amorphous hydrogenated silicon

Mark J. Kushner

University of Illinois, Department of Electrical and Computer Engineering, Gaseous Electronics Laboratory, 607 East Healey Street, Champaign, Illinois 61820

(Received 1 July 1987; accepted for publication 1 September 1987)

The surface processes during the plasma-enhanced chemical vapor deposition and reactive sputter deposition of amorphous hydrogenated silicon ($a\text{-Si:H}$) are investigated by use of a phenomenological model. The model consists of an accounting, in rate equation form, of adsorption of radicals from the plasma onto the surface, surface diffusion, incorporation into the lattice, interconnection of bonds in the lattice, and burial of species on the surface, thereby constituting film growth. By accounting for the coordination partners of Si atoms in the film, the atomic fraction of hydrogen in the film is computed for the lattice and for hydrogen in polymeric or isolated configurations. Results from the model are discussed while parametrizing the probability for hydrogen elimination during incorporation and the probability for saturation of dangling bonds by gas phase species. We find that the mode of hydrogen elimination during incorporation distinguishes films grown dominantly from SiH_2 or SiH_3 radicals. Characteristics of films grown by sputter deposition are investigated as a function of the composition of the radical flux. We find that films grown from hydrogen-rich fluxes are composed dominantly of dihydride ($\text{Si} < \text{H}$) configurations, whereas hydrogen-lean mixtures are composed of dominantly hydride (Si-H) configurations.

I. INTRODUCTION

Thin films of amorphous hydrogenated silicon ($a\text{-Si:H}$) are produced by a variety of means, including thermal chemical vapor deposition (CVD),¹ homogeneous chemical vapor deposition (HOMOCVD),² plasma-enhanced chemical vapor deposition (PECVD),³ and reactive sputter deposition (RSD).⁴ The films thus produced typically have atomic hydrogen fractions of 5%–20%, and thicknesses of $\approx 0.5\ \mu\text{m}$ for use in electronic devices and 10–15 μm for use as photoreceptor material.⁵ Of the methods of fabrication listed above, the former two rely upon thermal pyrolysis of gaseous silane compounds (e.g., SiH_4 , Si_2H_6) to generate the radicals from which the film is grown; the latter two methods generate the radicals by electron or ion impact processes. The purpose of this paper is to theoretically investigate the property of $a\text{-Si:H}$ films produced by the latter two methods.

The apparatus typically used for PECVD is a parallel-plate capacitively coupled radio-frequency discharge sustained in mixtures of silane (or disilane), hydrogen, and noble gases at pressures $< 0.5\ \text{Torr}$.^{6,7} The substrate temperature is typically 400–700 K. Silicon-containing radicals (e.g., SiH_2 , SiH_3) are generated by electron impact dissociation of the feed stock at discharge power levels of tens to hundreds of mW cm^{-2} . The radicals then diffuse out of the plasma to the substrate where they are incorporated into the growing film. The apparatus typically used for RSD is functionally similar to that for PECVD, except that one of the electrodes (the target) is covered by a silicon plate, and the gas pressure is lower ($< 0.1\ \text{Torr}$).⁸ Noble gas ions from the discharge impact into the target, thereby sputtering Si atoms, which then drift to, and deposit on, the substrate, typically the opposite electrode. By flowing controlled amounts of hydrogen through the sputter chamber, the frac-

tion of hydrogen incorporated into the film can be controlled.⁵ Additional control of the amount of incorporated hydrogen in the film is obtained in both methods by regulating the substrate temperature; the higher the substrate temperature, the lower the hydrogen fraction.

The processes through which radicals generated by the plasma during PECVD and RSD are adsorbed onto the surface and incorporated into the film are complex, and the study of those processes are current topics of research.^{2,5,9–15} The processes can be divided into the following general categories: adsorption, incorporation, hydrogen elimination, interconnection, etching, sputtering, and burial. Adsorption is the process whereby radicals from the plasma stick to the surface and become available for bonding to the film. Incorporation is the process whereby a radical on the surface covalently bonds to another silicon atom in the film. We call this bonding to the lattice, although the use of the term lattice does not claim any long-term order. Incorporation can be direct, in which a radical attaches to the lattice at the site of a dangling bond; or indirect, in which the radical displaces hydrogen from saturated bonds (i.e., Si-H), thereby eliminating hydrogen from the surface. Etching is the process whereby radicals remove atoms from the lattice or remove adsorbed species by colliding and bonding to those species but not sticking on the surface. Sputtering is the analogous process performed by energetic ions colliding with the surface. Burial is the process during which interconnection and incorporation cover over atoms previously on the surface and exposed to the plasma, and confine them to the lattice.

The fraction of hydrogen in $a\text{-Si:H}$ films, 5%–20%, is small compared to the ratio of hydrogen to silicon atoms in the flux of radicals which adsorb or collide with the growing film. The manner in which the excess hydrogen is eliminated

is therefore an important consideration. Heuristic models for growth of *a*-Si:H films by PECVD have been suggested by Kampas,⁹ Scott, Reimer, and Longeway,¹¹ Longeway,¹⁴ Gallagher,¹⁵ and others. These models differ qualitatively in the manner in which hydrogen is eliminated from the film. Kampas⁹ suggests that cross linking between adjacent Si-H bonds on the surface resulting in elimination and desorption of H₂ is the dominant mechanism. Scott¹¹ also suggests that hydrogen atoms are removed from Si-H bonds on the surface via etching reactions by radicals from the plasma. Another suggested method is that radicals (e.g., SiH₃) bond to the lattice as activated silyl groups, which spontaneously eliminate H₂ as a method of relaxation. Gleason *et al.*¹⁶ have recently published a Monte Carlo simulation for thin-film growth of *a*-Si:H. In their model the initiating step (called the addition reaction) proceeds by incorporation of SiH₄ directly into the film with the simultaneous elimination of H₂. This step resembles heterogeneous pyrolysis, and therefore the model is most directly applicable to CVD (as opposed to PECVD). In their model, though, hydrogen is eliminated from the film by cross linking between adjacent ≡Si-H bonds, in a manner similar to that suggested by Kampas.⁹

In this paper a phenomenological model for the surface deposition kinetics during PECVD and RSD of *a*-Si:H is presented, and results from the model are discussed for a variety of plasma conditions. The model consists of a set of rate equations describing the major processes of adsorption, surface diffusion, incorporation, interconnection, hydrogen elimination, and burial. From the results of the model, one obtains the fraction of hydrogen in the film, and the distribution of hydride (≡Si-H) and dihydride (≡Si $\overset{\text{H}}{\text{H}}$) bonds in the film. The model is described in Sec. II after which rate constants used in the model are discussed in Sec. III. Results from the model are presented in Sec. IV in the subtopics of hydrogen elimination during incorporation, the burial effect, saturation and etching, temperature effects, reactive sputter deposition, and deposition in the absence of SiH₃ insertion. Concluding remarks are in Sec. V.

II. DESCRIPTION OF THE MODEL

A model for gas phase chemical kinetics can be formulated by defining a set of species and rates, and expressing them as a set of rate equations. The rate equations have the general form

$$\frac{dN_i}{dt} = \sum_{l,m} N_l N_m k_{lm}^i - N_i \sum_{l,m} N_l k_{il}^m, \quad (1)$$

where k_{lm}^i is the rate constant for formation of species N_i by collisions between species N_l and N_m . The terms on the right-hand side of Eq. (1) simply represent the sources and sinks for species N_i . The surface deposition model (SDM) described in this paper consists of a set of rate equations similar to that which one would write for gas phase chemistry. There are six classes of species in the model. Allowing X to denote some specific species, the six classes are the following: $X(F)$, the flux of radicals incident onto the surface; $X(A)$, adsorbed nonmobile radicals; $X(M)$, adsorbed mobile radicals; $X(G)$, desorbed gas phase molecules; $X(L)$, a

silicon atom bounded to the lattice in the film but residing on the surface; and $X(B)$, a silicon atom bonded to the lattice in the film and buried beneath the surface.

The individual species in each class described above are listed in Table I. The species $X(L)$ and $X(B)$ represent silicon atoms on and below the surface. The relative densities of species in class $X(B)$ contain the information from which the fractions of hydrogen and silicon in the film are obtained and the types of bonds in the film are calculated. This information is obtained by tagging the silicon atoms $X(L)$ and $X(B)$ with their coordination partners. For example, SSSH(B) represents a silicon atom that is part of the lattice and buried beneath the surface. It is bonded to three other silicon atoms (SSS) and a hydrogen atom (H). SSHD(L) represents a silicon atom on the surface bonded to two silicon atoms (SS), one hydrogen atom (H) and having one dangling bond (D). The atomic fractions of hydrogen and silicon in the film are obtained by summing the silicon and hydrogen bonds of the buried silicon atoms and taking the appropriate ratios.

The following conceptual sequence of events is simulated by the SDM. Radicals are generated in the gas phase by electron impact and molecular reactions, and diffuse towards the surface. The composition of the radical flux is either specified as part of a parametric study or obtained from the results of a companion plasma chemistry model for rf discharges in silane gas mixtures.¹⁷ The radicals then adsorb on the surface as mobile adsorbates [$X(M)$], or etch or saturate the surface (see below). As energetically allowed, sputtering by ions directed towards the surface may also occur. Adsorbed mobile radicals diffuse on the surface. These radicals thermally desorb from an immobile state and readorb to the immobile state desorbing many times before colliding with a bonding site in the lattice on the surface [e.g., SSSD(L)]. At that time it is incorporated into the lattice, and hydrogen may be eliminated from the surface in the manner described below. Mobile radicals which collide and react with other mobile radicals may desorb from the surface as saturated molecules [e.g., SiH₃(M) + SiH₃(M) → Si₂H₆(G)]. Heterogeneous production of saturated molecules in this fashion is believed to be an important contribution to the density of gas phase species.^{10,15} Once a member of the lattice, further reactions, such as interconnection, may take place between adjacent silicon atoms. The silicon atoms on the surface are gradually buried [i.e., SSSH(L) → SSSH(B)] at a rate determined by the magnitude of the

TABLE I. Species included in the surface deposition model.

Surface and lattice species [$X(L)$, $X(B)$]	Radical flux, adsorbed, and buried isolated species [$X(F)$, $X(M)$, $X(A)$, $X(B)$]
SSSS	H Si SiH SiH ₂ SiH ₃
SSSD SSSH	Si ₂ H ₂ Si ₂ H ₃ Si ₂ H ₄ Si ₂ H ₅
SSDD SSHD SSSH	
SDDD SHDD SHHD SHHH	
Saturated gas phase species [$X(G)$]	
H ₂ SiH ₄ Si ₂ H ₆	

flux of radicals incident onto the surface and by the requirement that the total density of surface species remains a constant. Burial is distinct from interconnection. Radicals on the surface may interconnect; however, they are not buried beneath the surface unless there is a flux of radicals to cover them.

There are two types of surface sites. The first site is the location at which a silicon atom bonds to the lattice; the second site is a location at which a radical is immobily adsorbed. The density of bonding sites, ρ_0 is a^{-2} , where a is the average bond length, taken to be 2.75 Å. The density of adsorption sites was assumed to be $0.5\rho_0$. The distinction between mobile and immobile adsorbed radicals is that mobile radicals are free to diffuse along the surface. Immobile adsorbed radicals are confined to their adsorption sites, but they may thermally desorb and become mobile. Mobile and immobile adsorbed radicals were invoked to account for the observation that hydrogen in α -Si:H films produced by PECVD is contained in both the lattice and in isolated polymeric configurations, $(\text{SiH}_2)_n$.^{7,12} We attribute the isolated configurations to clusters of adsorbed SiH_n molecules which the film has grown over and buried, but which are not incorporated (i.e., bonded) to the lattice.

Rate equations were formulated for the processes described above using the coordination partner notation to account for bond densities. For example, the interconnection of dangling bonds of two adjacent silicon atoms on the surface is represented schematically as



The contribution of this process to the rate equations is simply $[\text{SSH}(L)][\text{SSSD}(L)]k$, where $[X]$ is the surface density of the species and k is the reaction rate constant. A set of sample reactions appear in Table II. All energetically allowed combinations of reactants from Table I for the sample reactions were included in the model.

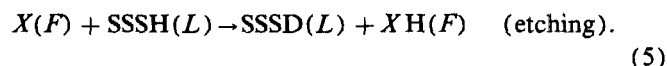
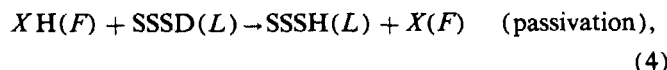
III. REACTION RATE CONSTANTS

Reaction rate constants are required for all the processes described above; adsorption, desorption, surface diffusion, lattice building, interconnection, and burial. Although some of these rates are known for crystalline silicon, such as the adsorption probability,¹⁸ they are generally not

known for amorphous silicon, particularly when dangling bonds on the surface may be passivated by hydrogen. Therefore, the rate constants must be estimated in an internally consistent fashion, as described below.

A. Adsorption, passivation, and etching

This category of reactions includes processes involving the flux of radicals or molecules from the plasma. These reactions are represented schematically, or by example, by



Since the values of $X(F)$ in the SDM are specified parameters and are nearly independent of the surface processes (see below), their densities are constants in the expressions above. The time rate of change of the density of a surface species, $X(L)$, expressed as $\text{cm}^{-2} \text{s}^{-1}$, for process j involving $X(F)$ is therefore $[X(F)]p_j[X(L)]/\rho_0$, where p_j is the probability of the process and $[X(L)]/\rho_0$ is the fractional surface coverage of the reactant surface species. For adsorption, the fractional surface coverage is set to unity so that the rate of adsorption depends only on the probability p_j . We treat p_j as a parameter in the model.

B. Mobile and immobile adsorbed radicals

Mobile radicals $X(M)$ are immobilized by "colliding" with an active adsorption site. Since the adsorption site can be considered equivalent to a lattice site, the rate of immobile adsorption is as given in the next section. The rate of desorption for $X(A) \rightarrow X(M)$ is $\nu_d e^{-(\Delta\epsilon_d/kT_s)}$, where ν_d is the desorption frequency, T_s is the substrate temperature, and $\Delta\epsilon_d$ is the adsorption energy. By parametrizing the results of the model for the hydrogen fraction in isolated configurations as a function of surface temperature (see below), and comparing to experiment,⁷ we estimated that $\nu_d = 10^5 \text{ s}^{-1}$ and $\Delta\epsilon_d = 0.2 \text{ eV}$.

TABLE II. Exemplary reactions included in the model (see text for rates).^a

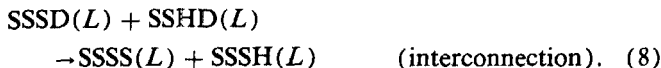
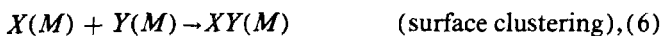
$\text{SiH}_2(F) \rightarrow \text{SiH}_2(M)$	Adsorption to mobile state
$\text{SiH}_2(M) \rightleftharpoons \text{SiH}_2(A)$	Mobile adsorption \rightleftharpoons Immobile desorption
$\text{SiH}_2(F) + \text{SSSH}(L) \rightarrow \text{SiH}_3(F) + \text{SSSD}(L)$	Etching
$M^+(F) + \text{SSSH}(L) \rightarrow M(F) + \text{SSSD}(L) + H(G)$	Sputtering ^b
$\text{SiH}_3(F) + \text{SSSD}(L) \rightarrow \text{SiH}_2(F) + \text{SSSH}(L)$	Saturation
$\text{SiH}_3(M) + \text{SiH}_3(M) \rightarrow \text{Si}_2\text{H}_6(G)$	Surface clustering and desorption
$\text{SiH}_2(M) + \text{SSSD}(L) \rightarrow \text{SSSS}(L) + \text{SSHH}(L)$	Incorporation
$\text{SiH}_3(M) + \text{SSSH}(L) \rightarrow \text{SSSS}(L) + \text{SHHD}(L) + \text{H}_2(G)$	Incorporation with H_2 elimination
$\text{SSSD}(L) + \text{SSSD}(L) \rightarrow \text{SSSS}(L) + \text{SSSS}(L)$	Interconnection
$\text{SSSH}(L) + \text{SSSH}(L) \rightarrow \text{SSSS}(L) + \text{SSSS}(L) + \text{H}_2(G)$	Interconnection with H_2 elimination
$\text{SSSH}(L) \rightarrow \text{SSSH}(B)$	Burial (lattice species)
$\text{SiH}_2(A) \rightarrow \text{SiH}_2(B)$	Burial (isolated configurations)

^a All allowed permutations of exemplary reactions for the species listed in Table I are included in the model.

^b M^+ denotes any energetic ion incident onto the surface.

C. Surface clustering, lattice building, and interconnection

The reactions in this category have the general or exemplary form of



The time rate of change of a surface species resulting from process j in this category is $[X][Y]k_j p_j e^{-(\Delta\epsilon/kT_s)}$, where $[X]$ and $[Y]$ are the densities of the reactants (cm^{-2}), k_j is the rate constant ($\text{cm}^2 \text{s}^{-1}$), $\Delta\epsilon_j$ is an activation energy, and p_j is a relative probability of the process. For processes involving reactants that are both lattice species, $p_j = 1$. For processing where one of the reactions is a mobile species, and therefore diffusing on the surface, $p_j = \{(T_s/500 \text{ K}) \times [M/(2\mu)]\}^{1/2}$, where M is the molecular weight of $\text{SiH}_3(M)$ and μ is the reduced mass of the reactants. This scaling parameter merely accounts for lighter adsorbates having a higher thermal velocity and therefore a higher probability for reaction per unit time. Unless otherwise noted, for reactions between adsorbed species, or adsorbed species and the lattice, k_j ($T_s = 500 \text{ K}$) = $1.5 \times 10^{-12} \text{ cm}^2 \text{ s}^{-1}$ and $\Delta\epsilon = 0$ (see below). For interconnection reactions between saturated lattice species [i.e., $\text{SSSH}(L)$], $k_j = 3.0 \times 10^{-8} \text{ cm}^2 \text{ s}^{-1}$, and $\Delta\epsilon$ is either 1.5 or 10 kcal/mol (see below).

For unity coverage of reactants, the reaction frequency is approximately 2000 s^{-1} . The average time a radical is immobile adsorbed ($T_s = 500 \text{ K}$) is 0.75 ms. Therefore, radicals spend little time in the mobile state, but rather move from immobile site to immobile site or to an incorporation site. The results of the model are relatively insensitive to the choice of k_j provided that the reaction frequency is comparable to or larger than the desorption frequency. The values for rate constants were obtained by parametrically comparing the results of this model to the experimental results of Ross and Jaklik.⁷ The values derived are not unique and are merely intended to represent general reaction probabilities.

The activation energies $\Delta\epsilon$ were estimated for each reaction by assigning bond energies and computing the change in total energy going from reactants to products. Exothermic reactions were assigned zero activation energies; endothermic reactions were assigned an activation energy equal to the endothermicity. The bond energies for surface configurations were estimated from the work of Ho *et al.*¹⁹ who calculated a correction factor for Si-Si and Si-H bond energies in higher silane molecules. In general, all clustering, insertion, and lattice building reactions involving species having dangling bonds are exothermic to the degree of approximation of this method. The endothermic reactions have energies on the order of a few to 10 kcal/mol. These reactions are primarily lattice interconnection with molecular hydrogen elimination. The activation energy associated with these reactions is responsible, in part, for the observed reduction in the f_H with increasing substrate temperature.^{7,11,20,21} We assigned an activation energy of 1.5 kcal/mol for interconnection re-

actions involving the lattice species $\text{SSSH}(L)$; and 10 kcal/mol for reactions involving $\text{SSHH}(L)$ and $\text{SHHH}(L)$. This difference in activation energies will be discussed in Sec. IV D.

The rate of interconnection between dangling bonds [e.g., $\text{SSSD}(L) + \text{SSSD}(L) \rightarrow \text{SSSS}(L) + \text{SSSS}(L)$] is calculated during execution of the model. The instantaneous rate is chosen so that upon burial, the fractional density of dangling bonds is $< 1\%$. The rate so derived varies from case to case, but is generally close to $2-5 \times 10^{-12} \text{ cm}^2 \text{ s}^{-1}$. Although the spin density in $\alpha\text{-Si:H}$ is usually much less than 0.01, we found that requiring a smaller density than this upon burial, that is, having a higher rate of interconnection, resulted in unphysically small hydrogen fractions. The implication of this observation is that interconnection between dangling bonds continues in the film after burial.¹¹

C. Burial

Burial is the process whereby species residing on the surface are incorporated into the film. For lattice species, this is schematically shown, for example, as



The rate of burial for surface species $X_j(L)$ is $(X_j(L)/\rho_0) \times (\rho_L - \rho_0)/\tau$ for $\rho_L > \rho_0$, and zero otherwise, where $\rho_L = \sum_j X_j(L)$ is the sum of all lattice species and τ is the burial equilibration time. This rate "clamps" the density of surface lattice species at ρ_0 . The model is not sensitive to the choice of τ as long as $\tau \ll \rho_0 / [\sum_j n_j X_j(F)]$, where $X_j(F)$ is the net flux of radical species j that sticks on the surface and n_j is the number of silicon atoms contained in the radical. For very high deposition rates ($> 1000 \text{ \AA}/\text{min}$) the limiting value for τ is $\approx 150 \text{ ms}$; therefore, we used $\tau = 10 \text{ ms}$ for all cases.

D. Initial conditions

The initial conditions used for the model are that the surface is covered with dangling bonds [i.e., $\text{SSSD}(L)$] having density ρ_0 , and unoccupied adsorption sites having density $0.5\rho_0$. The fluxes are turned on and the rate equations are integrated until steady-state conditions are reached. We found that for constant fluxes, final surface conditions were obtained in 1-3 s of real time, corresponding to only 5-10 "monolayers" of film, and that the hydrogen content decreased to its steady-state value. These observations agree well with the results of Gleason *et al.*,¹⁶ who calculated that steady-state conditions are obtained after depositing a similar number of monolayers, and hydrogen content decreases towards its steady-state value. We have also started with a prepared surface [e.g., a partial covering of $\text{SSSH}(L)$]; and found little or no change in the steady-state results when compared to starting with a fresh surface.

IV. RESULTS

In the plasmas of interest, the dominant radicals are thought to be SiH_2 and SiH_3 .^{22,23} The ratio of hydrogen atoms to silicon atoms in silicon-containing radicals incident onto the surface, $[H]/[Si] = F_H$, is therefore approximately 2-3. The electron impact dissociation of saturated silanes which generated the radicals also generate a nearly equal

density of atomic hydrogen. The flux of hydrogen atoms incident onto the surface is therefore larger (6–8) than the value given by the silicon-containing radicals alone. Additional hydrogen is deposited on the surface by hydrogen-containing molecules from the gas phase which saturate dangling bonds, as discussed below. The fraction of hydrogen incorporated into the film, f_H , though, is usually ≤ 0.20 . Therefore, hydrogen must be eliminated from the surface some time between the processes of adsorption and burial; or once buried, hydrogen must be eliminated from the lattice. In this work we examine the former process. We assumed that hydrogen, once buried beneath the surface, is permanently part of the film.

In the results discussed below, we either specify the radical flux as part of a parametric survey or use the flux computed with the plasma chemistry model. By specifying a flux, we ignore the effect of surface chemistry on the radical flux. Since the majority of the desorbed products of the surface chemistry are saturated molecules, this effect is small.

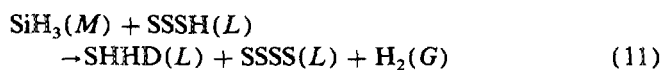
A. Hydrogen elimination during incorporation

When adsorbed molecules are incorporated into the lattice, they attach to either dangling bonds [e.g., SSSD(L)] or insert into saturated bonds [e.g., SSSH(L)]. Any adsorbed radical may incorporate directly into a site occupied by a dangling [e.g., $\text{SiH}_3(M) + \text{SSSD}(L) \rightarrow \text{SSSS}(L) + \text{SHHH}(L)$]. Incorporation by insertion into a saturated bond, though, may necessarily require elimination of hydrogen. For purposes of identification, we label the adsorbed radical by its ratio of hydrogen to silicon atoms, $F_H = [\text{H}]/[\text{Si}]$. For $F_H < 2$, adsorbed radicals may insert directly into saturated SSSH(L) bonds without eliminating hydrogen; for example,



For adsorbed radicals having $F_H > 2$, the insertion reaction requires elimination or displacement of hydrogen. Elimination may proceed by displacing atomic or molecular hydrogen. This method of incorporation of radicals having $F_H > 2$ is the analogy of the gas phase reaction $\text{SiH}_3 + \text{SiH}_4 \rightarrow \text{Si}_2\text{H}_5 + \text{H}_2$ which, at typical substrate temperatures, proceeds with a rate constant of $\approx 10^{-13} \text{ cm}^3 \text{ s}^{-1}$.²⁴ If radicals having a single dangling bond [e.g., $\text{SiH}_3(M)$] are unable to insert into a saturated surface site [e.g., SSSH(L)], then incorporation can only proceed by generating dangling bonds on the surface by sputtering or etching mechanisms.¹⁵ In this section we investigate surface deposition while allowing insertion of $\text{SiH}_3(M)$ into saturated surface sites. In Sec. V F we examine some of the consequences of requiring a dangling bond for incorporation of $\text{SiH}_3(M)$ into the lattice.

For the incorporation of $\text{SiH}_3(M)$ while allowing insertion into saturated surface sites, we may have either of^{9,15}



The former reaction is thermodynamically favored. If it is more likely to occur, the elimination of molecular hydrogen during incorporation of $\text{SiH}_3(M)$ into films grown from

plasmas whose predominant radical is $\text{SiH}_3(F)$ may result in less hydrogen remaining on the surface than incorporation of $\text{SiH}_2(M)$, a radical having a smaller value of F_H .

Before examining the results of the model for actual discharge conditions, it is instructive to examine the characteristics of *a*-Si:H films grown from specific fluxes of radicals. We will examine the fraction of incorporated hydrogen, f_H , as a function of the hydrogen-to-silicon ratio F_H of the individual radicals incident on to the surface. This is accomplished by specifying that the radical flux is composed of only a single specie having a given F_H . These results are shown in Fig. 1 where f_H is plotted as a function of F_H while allowing adsorbed radicals with a single dangling bond to insert into a saturated surface site. The flux of silicon atoms incident on the surface was kept constant at $2 \times 10^{15} / \text{cm}^2 \text{ s}$, typical of moderately power discharges of tens to 100 mW/cm² sustained in a few hundred mTorr of SiH_4 and corresponding to a deposition rate of *a*-Si:H of $\approx 250 \text{ \AA}/\text{min}$. As expected, f_H increases with increasing F_H , but only to a ratio of $F_H \approx 2$ (as shown by the triangles in the figure), after which f_H decreases. This trend is a result of having H_2 (as opposed to H) being eliminated during incorporation of adsorbed radicals, that is, using the insertion step shown in Eq. (11) as opposed to that shown in Eq. (12). If we instead specify that H atoms are eliminated during incorporation (dashed line in Fig. 1), f_H differs little from the cases for elimination of H_2 for $F_H < 2$, but is larger than the previous cases for $F_H > 2$. For these conditions, f_H is equally determined by hydrogen elimination during interconnection of adjacent Si-H(L) bonds after incorporation, and hydrogen elimination during incorporation. The latter process can have a significant effect on f_H for plasmas dominated by radicals having $F_H > 2$.

The sensitivity of f_H on the mode of hydrogen elimination during incorporation is further illustrated in Fig. 2 where f_H is plotted for films grown from $\text{SiH}_2(F)$ and $\text{SiH}_3(F)$ as a function of the probability of eliminating H_2 .

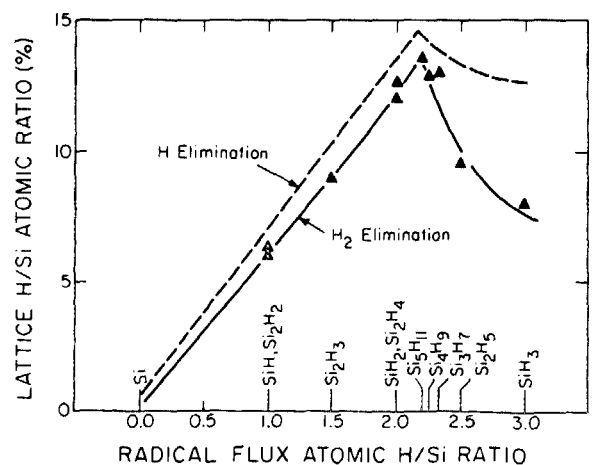


FIG. 1. Atomic fraction of hydrogen in *a*-Si:H films, f_H , as computed with the surface deposition model as a function of the H/Si ratio of individual radicals incident onto the surface. For these results, adsorbed radicals having a single dangling bond may insert into saturated surface sites. The triangles are for H_2 elimination during incorporation; the dashed line is for H atom elimination during incorporation.

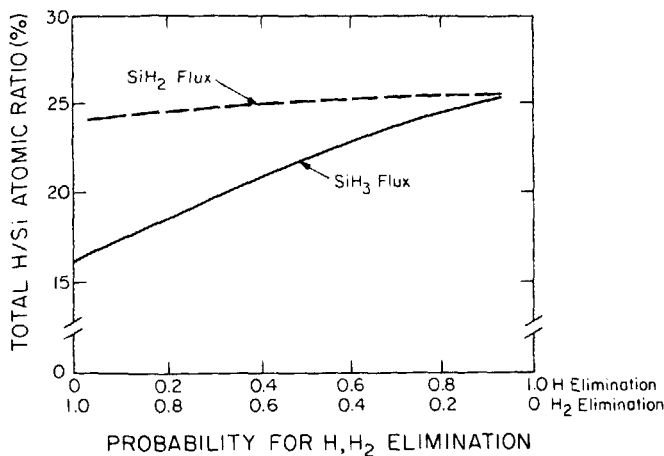


FIG. 2. Total hydrogen fraction (lattice and isolated) as a function of the probability of eliminating H_2 or H for incident fluxes of $SiH_2(F)$ and $SiH_3(F)$. A high probability for eliminating H_2 distinguishes between α -Si:H films grown from $SiH_2(F)$ and $SiH_3(F)$ when $SiH_3(M)$ insert into saturated surface sites.

The value of f_H for films grown from $SiH_2(F)$ is relatively insensitive to this probability, and when H atoms are eliminated there is little distinction between films grown from $SiH_2(F)$ and $SiH_3(F)$. As the probability of H_2 elimination increases, though, f_H decreases for films grown from $SiH_3(F)$.

Computed atomic hydrogen fractions in α -Si:H films for films grown in Ar/ SiH_4 rf discharges are shown in Fig. 3. The discharge conditions were simulated with the plasma chemistry model described in Ref. 17. The plasma conditions for these examples are as follows: gas pressure, 0.5 Torr; substrate temperature, 500 K; and power deposition, $\approx 25 \text{ mW cm}^{-3}$. Cases are shown for varying the fraction of SiH_4 in Ar. To eliminate the burial effect (see next section) the power for each case was varied to obtain the same deposition rate. Since the total atomic hydrogen fraction increases with decreasing fraction of SiH_4 while the deposition rate is constant, the change in f_H is a result of a change in the composition of the radical flux. Also plotted in Fig. 3 are the ratios of the total flux of H atoms to Si atoms incident on the surface, $[H]/[Si]$; and the ratio of radicals which have $F_H < 2$ to those having $F_H > 2$, $[Si_n H_n, n/m < 2]/[Si_n H_n, n/m > 2]$. Both ratios increase with decreasing fraction of silane. This trend is a consequence of silane radicals and hydrogen atoms, once generated by electron impact of silane, having a smaller probability of colliding with other silane molecules before striking the substrate as the silane fraction decreases. Of the two ratios, the latter, that comparing radicals having F_H greater than and less than 2, correlates better with f_H . The increase in f_H may therefore be caused, in part, by the effect shown in Fig. 1; radicals with $F_H > 2$ eliminate hydrogen during incorporation at a higher rate than those radicals having $F_H < 2$.

C. The burial effect

It has been generally observed that for a given gas mixture, f_H increases with increasing rate of deposition of α -Si:H.^{7,25,26} The deposition rate is usually increased by in-

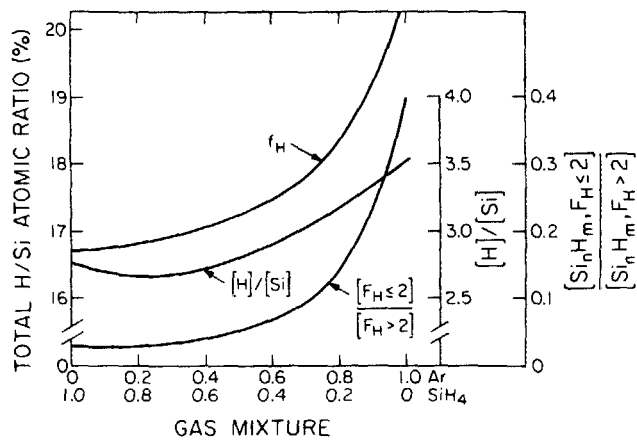


FIG. 3. Computed hydrogen fraction f_H and H/Si ratios in the incident flux as a function of gas mixture. $[H]/[Si]$ is the ratio of all hydrogen atoms to silicon atoms incident onto the surface; $[Si_n H_n, F_H < 2]/[Si_n H_n, F_H > 2]$ is the ratio of radicals that have $F_H = H/Si < 2$ and $F_H > 2$.

creasing discharge power. Therefore, the increase in f_H can result from either a change in the composition of the radicals incident on the surface or from what we call the burial effect. The burial effect is a physical, as opposed to a chemical, effect. The results of our model are consistent with lattice interconnection with molecular hydrogen elimination being a major method of removing hydrogen from the surface. To the extent that the rate of interconnection and hydrogen elimination is finite, the rate of hydrogen elimination is proportional to the residence time of adjacent $Si-H(L)$ bonds on the surface. The higher the rate of deposition, the shorter the residence time of $Si-H(L)$ bonds on the surface prior to burial and the smaller the probability that hydrogen is eliminated from the surface.

The burial effect is illustrated in Fig. 4, where we have plotted f_H as a function of deposition rate. Figure 4(a) shows results for idealized cases of the flux of radicals being composed of a single species. Figure 4(b) shows simulated results for and the experimental results of Ross and Jaklik.⁷ The simulated fluxes were generated with the model described in Ref. 17. In both cases f_H increases with increasing deposition rate. For these cases we allow insertion of $SiH_3(M)$ into $Si-H(L)$ with H_2 elimination. The lattice f_H for $SiH_3(F)$ is therefore less than that for $SiH_2(F)$ due to H_2 elimination during incorporation; f_H in isolated configurations is greater for $SiH_3(F)$ in the absence of this effect. Over the indicated range of power deposition, in the simulated results [Fig. 4(b)] the fractional composition of the radical flux changes by only a few percent. The dominant effect responsible for increasing f_H is the burial effect. For the results in Fig. 4, gas phase molecules did not saturate the surface. That effect will be discussed in the next section.

D. Saturation and etching of lattice bonds by gas phase molecules

The reaction of radicals and molecules from the plasma which collide with but do not adsorb on the surface are important because they can either remove hydrogen from (etch) the surface by removing a hydrogen atom from a $Si-$

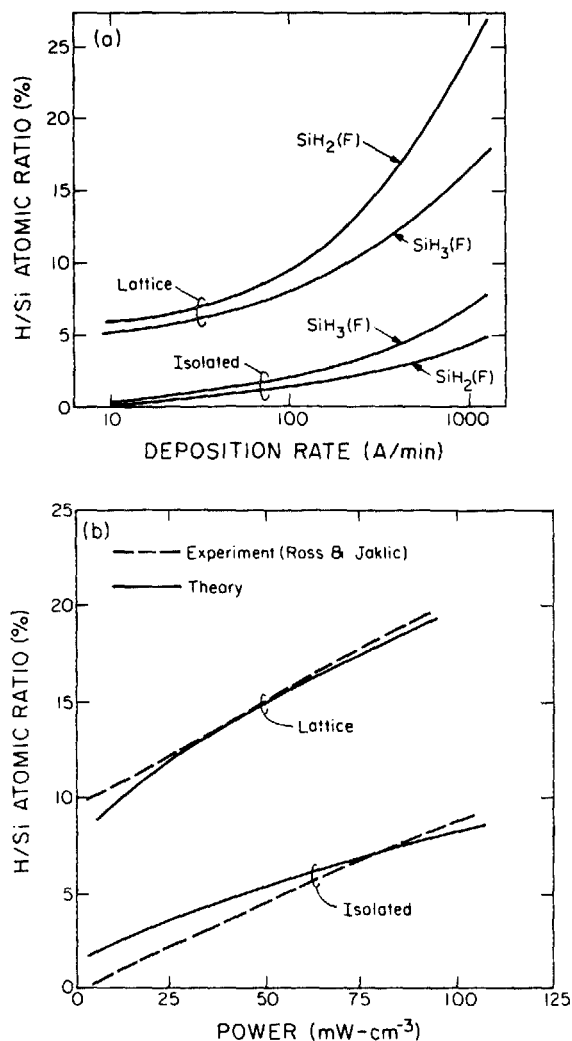


FIG. 4. Hydrogen atomic ratio in *a*-Si:H films as a function of discharge power, demonstrating the burial effect. (a) f_H for individual radical species, (b) this model's results and experimental values (Ref. 7) for deposition of *a*-Si:H from an rf discharge in SiH_4 .

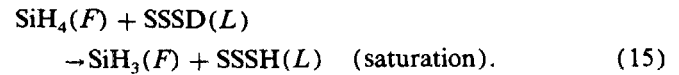
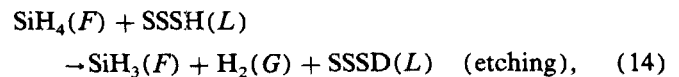
$\text{H}(L)$ bond, or deposit hydrogen on (saturate) the surface by inserting a hydrogen atom into a $\text{Si}-\text{D}(L)$ bond.¹⁵ An example of these two processes are the forward (etching) and reverse (saturation) reactions



Since a $\text{Si}-\text{H}(L)$ bond on the surface is exchanged for a $\text{Si}-\text{H}(F)$ bond in the gas phase radical, the exothermicity of the class of reactions with radicals is determined by the difference in bond energies for $\text{SiH}_n\text{H}(F)$ and $\text{SSS}-\text{H}(L)$. Robertson and Gallagher assigned a bond energy of ≈ 80 kcal/mol to $\text{SSS}-\text{H}(L)$.¹⁰ The $\text{SiH}_2-\text{H}(F)$ bond energy is approximately 75 kcal/mol. To the level of accuracy of the approximations, this class of reactions involving radicals can be considered thermoneutral. The equilibrium ratio of saturated bonds to dangling bonds, $[\text{SSSH}(L)]/[\text{SSSD}(L)]$, resulting from these processes involving radicals is therefore $[\text{SiH}_n(F)]/[\text{SiH}_{(n-1)}(F)]$. For typical plasma conditions²³ this ratio is > 10 , so that the equilibrium density of saturated to dangling bonds resulting from these radical reactions is $[\text{SSSH}(L)]/[\text{SSSD}(L)] > 10$. Therefore, surface

bonds are more likely to be saturated than etched by radicals via this process. Even though the steady-state density of dangling bonds made available by this process is likely to be small, the process may be an important source of dangling bonds for the case where adsorbed radicals as $\text{SiH}_3(M)$ cannot insert into saturated surface sites [e.g., $\text{SSSH}(L)$].¹⁵

Analogous etching and saturation reactions can also occur by collisions of saturated molecules with the lattice. Examples of these reactions are



The etching reaction in Eq. (14) is endothermic, since two $\text{Si}-\text{H}$ bonds are exchanged for the single $\text{H}-\text{H}$ bond. The saturation reaction in Eq. (15), though, is approximately thermoneutral in the same manner as for the analogous reaction involving radicals in Eq. (13). Since SiH_4 is the feed stock, the large ratio of densities of $[\text{SiH}_4(F)]/[\text{SiH}_3(F)]$ insures that the equilibrium density of saturated bonds compared to dangling bonds resulting from this process is large; the relative etching probability is small, although the contribution may be an important source of dangling bonds (see above). From this discussion, one can conclude that nonadsorbing gas phase radicals and molecules colliding with the growing film are more likely to contribute hydrogen to the surface than remove it.

The saturation of dangling bonds on the surface of the lattice by gas phase, nonadsorbing molecules clearly has the potential of being an important source of hydrogen to the film. We investigated this process by assigning a probability of saturating $\text{Si}-\text{D}(L)$ bonds with hydrogen resulting from collisions of $\text{SiH}_4(F)$ and $\text{H}_2(F)$, the saturated molecules having the largest flux striking the surface. The rate of saturation of dangling bond $X_j(L)$ was specified to be $p_s ([\text{SiH}_4(F)] + [\text{H}_2(F)]) [X_j(L)] / \rho_0$, where p_s is the saturation probability. The effect on f_H of varying p_s is shown in Fig. 5. The case shown is the same as in Fig. 4(b) for Ar/

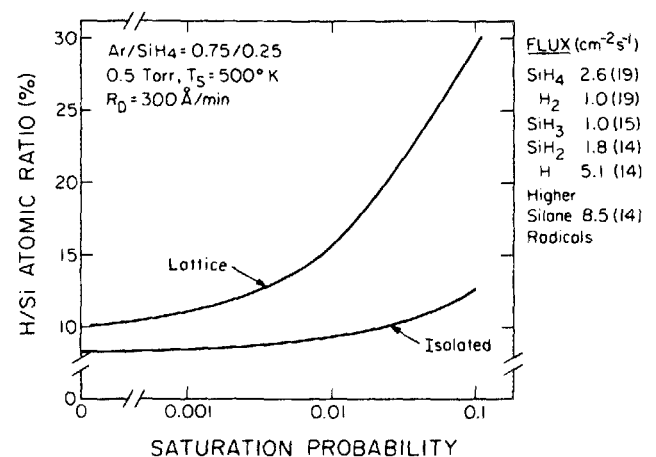


FIG. 5. Computed hydrogen atomic fraction as a function of the saturation probability of dangling bonds [e.g., $\text{SSSD}(L)$] by nonadsorbing molecules from the plasma (H_2 , SiH_4). The plasma conditions are the same as for Fig. 3. The partial composition of the radical and molecular flux to the surface is shown at right.

$\text{SiH}_4 = 0.75/0.25$. The composition of the flux is also shown in the figure. The fraction of incorporated hydrogen, f_H , increases significantly when the probability for saturation is $> 10^{-3}$.

The fraction of hydrogen in isolated configurations also increases with increasing lattice saturation probability, although to a lesser degree than f_H of the lattice. The increase of f_H in isolated configurations is due to the adsorbed mobile radicals $[X(M)]$ having a smaller probability of encountering a lattice site having a dangling bond when the saturation probability is high. Since incorporation of $X(M)$ into a saturated bond has a smaller rate constant, the residence time and density of $X(M)$ on the surface increases, thereby increasing the probability of being buried as an isolated configuration.

D. Substrate temperature

Computed hydrogen fraction f_H as a function of substrate temperature T_s for the experimental conditions of Ross and Jaklik⁷ appear in Fig. 6. f_H decreases with increasing substrate temperature due to the activation energy for interconnection and hydrogen elimination of Si-H(L) bonds. The activation energy derived here, 1.5 kcal/mol, is approximately equal to that empirically derived by measuring f_H as a function of T_s , 1.35 kcal/mol.¹¹ The decrease of hydrogen in isolated or polymeric configurations results from a decrease in the residence time of $\text{SiH}_x(A)$ as immobile adsorbates; a consequence of the activation energy for desorption.

The relative densities of hydrides and dihydrides is also a function of substrate temperature, as shown in Fig. 7. In this figure the experimental results of Luvcosky, Nemanich, and Knights¹² and results from the model for $[\text{SSSH}(B)]/[\text{SSHH}(B)]$ are plotted as a function of T_s and rf power (deposition rate).²⁷ The relative hydride density increases with increasing T_s and is nearly constant for discharge power greater than 5 W (deposition rate of 150 Å/min). To obtain these results, it was necessary to invoke a higher activation energy (10 kcal/mol) for interconnection and hydrogen elimination between di- and trihydride $[\text{SSHH}(L)$, $\text{SHHH}(L)]$ configurations than between hydride $[\text{SSSH}(L)]$ configurations (1.5 kcal/mol). If the method of hy-

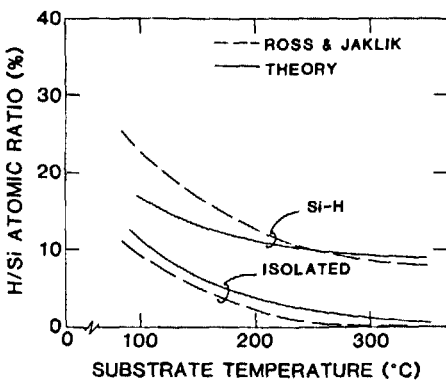


FIG. 6. Hydrogen atomic fraction as a function of substrate temperature as computed with the surface deposition model and the experimental results of Ross and Jaklik (Ref. 7).

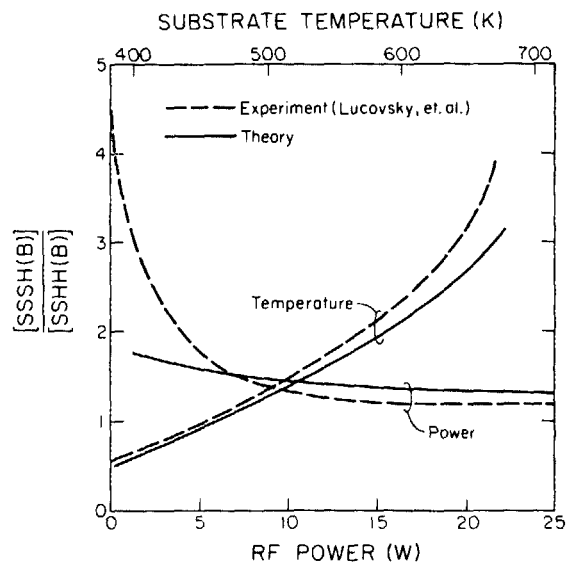


FIG. 7. The ratio of hydride $[\text{SSSH}(B)]$ and dihydride $[\text{SSHH}(B)]$ configurations in $a\text{-Si:H}$ films as calculated with the surface deposition model compared to the experimental results of Lucovsky *et al.* (Ref. 12). The two cases are for varying the rf power (deposition rate) and substrate temperature T_s . The relative hydride density increases with increasing T_s . To obtain agreement with experiment for the temperature dependence, two activation energies were invoked; for interconnection between hydrides, and for interconnection between di- and trihydrides.

drogen incorporation is a weak function of temperature, then a uniform activation energy for interconnection between all hydride configurations nets only a weak temperature dependence for their relative densities. It is possible that the difference in activation energies between hydrides and dihydrides lies not in the interconnection process but in the incorporation step. We assumed, though, that the latter process had no activation energy. The suggestion that activation energies for mono- and polyhydrides are different is consistent with the observation that above a substrate temperature of 575 K, hydrogen evolves from HOMOCVD films with a higher activation energy (30 kcal/mol) than below that temperature.¹¹

E. Reactive sputter deposition

Sputter deposition of $a\text{-Si:H}$ differs qualitatively from plasma deposition of $a\text{-Si:H}$ in that the operator, by adjusting target voltage and hydrogen flowrate, has finer control of the composition of radicals incident onto the substrate. Unlike PECVD, where a large fraction of the hydrogen incident onto the surface is contained in silane radicals, in reactive sputter deposition the hydrogen and silicon fluxes to the surface are dominantly atomic. For sputter deposition, the scaling parameter to characterize the incident flux is F_H^a , the ratio of atomic H(F) to atomic Si(F). The computed atomic hydrogen content of sputter deposited $a\text{-Si:H}$ is plotted in Fig. 8 as a function of F_H^a for three different substrate temperatures. The silicon flux is constant at $2.4 \times 10^{15} \text{ cm}^{-2} \text{ s}^{-1}$ corresponding to a deposition rate of 300 Å/min. As expected, the fraction of hydrogen in both the lattice and in isolated configurations increases with increasing F_H^a . At higher substrate temperatures, though, f_H for the lattice reaches a

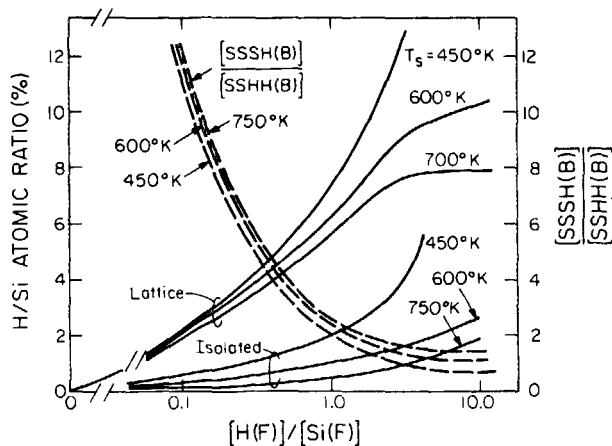


FIG. 8. Computed hydrogen atomic fraction and hydride/dihydride density for a -Si:H films grown by reactive sputter deposition as a function of the atomic hydrogen flux. The Si flux is constant at $2.4 \times 10^{15} \text{ cm}^{-2} \text{ s}^{-1}$, corresponding to a deposition rate of $300 \text{ \AA}/\text{min}$.

nearly constant value at $F_H^a \approx 2$, whereas f_H for isolated configurations continues to increase. The saturation of f_H is due in part, to an equilibration between adsorption and desorption of $\text{H}_2(\text{G})$ resulting from collisions between $\text{H}(\text{M})$ radicals; a process proportional to $[\text{H}(\text{F})]^2$ and which increases with increasing T_s .

The relative densities of hydride and dihydride configurations [i.e., $\text{SSSH}(\text{B})$ and $\text{SSHH}(\text{B})$] in the sputtered a -Si:H films are also plotted in Fig. 8. At low values of F_H^a , the films are composed of dominantly hydride [$\text{SSSH}(\text{B})$] configurations, and with increasing F_H^a , a larger fraction of hydrogen is contained in the film as dihydride [$\text{SSHH}(\text{B})$]. The cause for the increase in dihydride density with increasing F_H^a (at constant deposition rate) is analogous to the burial effect. Given a finite residence time of dangling bonds on the surface prior to burial, a higher flux of hydrogen passivates a larger fraction of those bonds, thereby leading to the higher dihydride density. If so, then at higher deposition rate (shorter residence time of dangling bonds on the surface) or higher substrate temperature (larger rate of interconnection), the ratio $[\text{SSSH}(\text{B})]/[\text{SSHH}(\text{B})]$ should decrease. This trend is confirmed by comparing the computed ratio $[\text{SSSH}(\text{B})]/[\text{SSHH}(\text{B})]$ to the experimental results of Jeffrey, Shanks, and Danielson⁸ in Fig. 9. For these results, the ratio $\text{H}(\text{F})/\text{Si}(\text{F})$ was obtained by normalizing to the experiment at a deposition of $\approx 330 \text{ \AA}/\text{min}$ [$\text{H}(\text{F})/\text{Si}(\text{F}) = 3$]. Results as a function of deposition rate were then obtained both while holding $\text{H}(\text{F})$ constant and assuming $\text{H}(\text{F})$ was proportional to the change in discharge power, which is directly proportional to deposition rate.

F. Deposition without insertion of $\text{SiH}_3(\text{M})$ into saturated surface sites

The details of the method of incorporation of $\text{SiH}_3(\text{M})$ into the lattice are particularly important, because $\text{SiH}_3(\text{F})$ has the highest flux of silicon containing radicals incident onto the surface. In Sec. V A we discussed the implications of having $\text{SiH}_3(\text{M})$ incorporate into the lattice by inserting

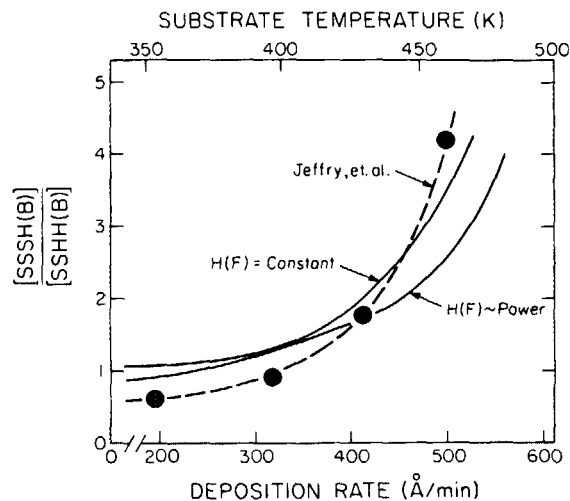


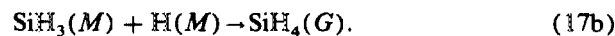
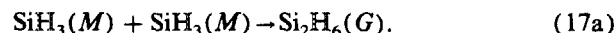
FIG. 9. Computed and experimental results for the ratio of hydride [$\text{SSSH}(\text{B})$] to dihydride [$\text{SSHH}(\text{B})$] density in a -Si:H films grown by reactive sputter deposition. The experimental results are from Jeffrey *et al.* (Ref. 8). The ratio of atomic H/Si of the radical flux for the model was obtained by normalizing to the experimental results at a deposition rate of $330 \text{ \AA}/\text{min}$. Two cases are shown, scaling H/Si with deposition rate (discharge power) and holding the hydrogen flux constant.

into Si-H(L) bonds and eliminating hydrogen, as in reactions (11) and (12). In this section we will discuss the implications of $\text{SiH}_3(\text{M})$ incorporation in the absence of this mechanism. For these conditions, $\text{SiH}_3(\text{M})$ can only be incorporated into the lattice at a surface site having a dangling bond, as in the reaction



The dangling bonds at surface sites are made available by etching [reactions (13) and (14)] or sputtering by bombardment of the surface with energetic ions (see Table II).

When $\text{SiH}_3(\text{M})$ cannot insert into Si-H(L) bonds, the rate at which $\text{SiH}_3(\text{M})$ incorporates into the lattice is smaller since the availability of the necessary surface sites [e.g., $\text{SSSD}(\text{L})$] is also smaller. For a constant $\text{SiH}_3(\text{F})$ flux, the surface density of $\text{SiH}_3(\text{M})$ therefore increases. Surface clustering and desorption reactions therefore also become more likely (see Table II.) The two desorption reactions which are important are



As a result of these reactions, the effective sticking coefficient for $\text{SiH}_3(\text{M})$ is less than unity.

We investigated the characteristics of a -Si:H films when $\text{SiH}_3(\text{M})$ incorporation occurs only via a dangling bond. These results are shown in Fig. 10 where the film deposition rate and effective sticking coefficient for $\text{SiH}_3(\text{M})$ are plotted as a function of the rate of generation of dangling bonds. The flux of radicals incident onto the surface have the ratio $\text{SiH}_3/\text{SiH}_2/\text{H} = 100/5/10$ with $[\text{SiH}_3(\text{F})] = 10^{16} \text{ cm}^{-2} \text{ s}^{-1}$. These values are typical for a low-powered plasma in a $\text{SiH}_4/\text{H}_2 = 1/1$ gas mixture at 0.25 Torr. The independent variable is the number of dangling bonds generated on the surface by sputtering or etching as a fraction of the $\text{SiH}_3(\text{F})$ flux incident onto the surface. As the rate of generation of

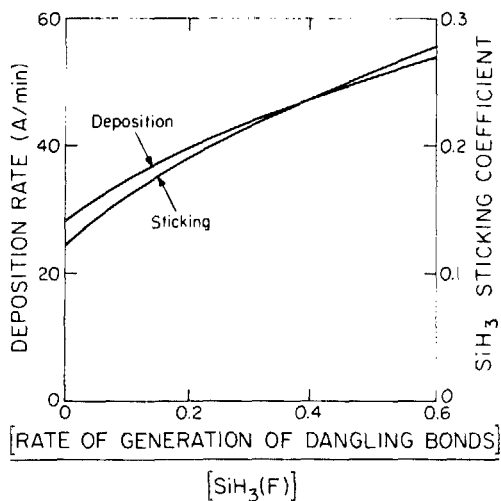
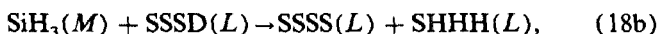
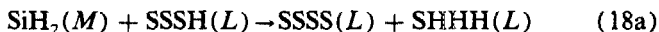


FIG. 10. Deposition rate and effective sticking coefficient for $\text{SiH}_3(M)$ as a function of the rate of generation of dangling bonds. For these results, $\text{SiH}_3(M)$ does not insert into $\text{Si-H}(L)$. The discharge conditions are $\text{SiH}_3(F)/\text{SiH}_2(F)/\text{H}(F) = 100/5/10$ with $\text{SiH}_3(F) = 10^{16} \text{ cm}^{-2} \text{ s}^{-1}$. The rate of generation of dangling bonds is expressed as a fraction of $\text{SiH}_3(F)$.

dangling bonds increases and the number of sites available for $\text{SiH}_3(M)$ insertion increases, both the deposition rate and effective sticking coefficient of $\text{SiH}_3(F)$ also increase. Over the range investigated, though, there is little change in hydrogen fraction ($9.5\% < f_{\text{H}} < 10.0\%$). This last observation is explained by the fact that if a dangling bond is required for incorporation of $\text{SiH}_3(M)$, then the two reactions responsible for deposition for these conditions,



are functionally equivalent with respect to "hydrogen accounting." The $\text{SiH}_3(M)$ which does not stick is desorbed primarily as disilane, as the desorption products have the ratio $[\text{Si}_2\text{H}_6(G)]/[\text{SiH}_4(G)] = 6$.

VI. CONCLUDING REMARKS

A phenomenological model for surface kinetics during plasma and sputter CVD of amorphous hydrogenated silicon has been described. The model consists of an accounting, in rate equation form, of adsorption, incorporation, interconnection, and other pertinent processes. The model has successfully compared with experimental results for hydrogen fraction and distribution of bond types. We found that molecular hydrogen elimination during incorporation distinguishes between films grown from plasmas whose primary radicals SiH_n have $n < 2$ or $n > 2$. We also found that the observed increase in hydrogen fraction with increasing deposition rate is largely a physical, as opposed to chemical, process. At higher deposition rates, the shorter residence time of $\text{Si-H}(L)$ bonds on the surface results in a smaller probability for interconnection and hydrogen elimination.

The cause for the increase in the fraction of hydrogen contained in hydride, as opposed to dihydride, configurations with increasing substrate temperature may be a result of there being a higher activation energy of interconnection between dihydride configurations.

ACKNOWLEDGMENT

This work was supported by the Materials Science Division of the Army Research Office under the direction of Dr. Andrew Crowson, Contract No. DAAG29-85-C-0031.

- ¹M. Hirose, in *Semiconductors and Semimetals*, edited by J. I. Pankove (Academic, Orlando, 1984), Vol. 21A, p. 109.
- ²B. A. Scott, R. M. Plecenik, and E. E. Simonyi, *Appl. Phys. Lett.* **39**, 73 (1981).
- ³M. Hirose, in *Semiconductors and Semimetals*, edited by J. I. Pankove (Academic, Orlando, 1984), Vol. 21A, p. 9.
- ⁴T. D. Moustakas, in *Semiconductors and Semimetals*, edited by J. I. Pankove (Academic, Orlando, 1984), Vol. 21A, p. 55.
- ⁵J. A. Thornton, in *Amorphous Metals and Semiconductors*, edited by P. Maasen and R. I. Jaffee (Pergamon, New York, 1986), pp. 299-314.
- ⁶P. E. Vanier, J. F. Kampas, R. R. Corderman, and G. Rajeswaran, *J. Appl. Phys.* **56**, 1812 (1984).
- ⁷R. C. Ross and J. Jalik, Jr., *J. Appl. Phys.* **55**, 3785 (1984).
- ⁸F. R. Jeffery, H. R. Shanks, and G. C. Danielson, *J. Appl. Phys.* **50**, 7034 (1979).
- ⁹F. J. Kampas, in *Semiconductors and Semimetals*, edited by J. I. Pankove (Academic, Orlando, 1984), Vol. 21A, p. 153.
- ¹⁰R. Robertson and A. Gallagher, *J. Chem. Phys.* **85**, 3623 (1986).
- ¹¹B. A. Scott, J. A. Reimer, and P. A. Longeway, *J. Appl. Phys.* **54**, 6853 (1983).
- ¹²G. Lucovsky, R. J. Nemanich, and J. C. Knights, *Phys. Rev. B* **19**, 2064 (1979).
- ¹³C. C. Tasi, J. C. Knights, G. Chang, and B. Wacker, *J. Appl. Phys.* **59**, 2998 (1986).
- ¹⁴P. A. Longeway, in *Semiconductors and Semimetals*, edited by J. I. Pankove (Academic, Orlando, 1984), Vol. 21A, p. 179.
- ¹⁵A. Gallagher, in *Materials Issues in Amorphous Semiconductor Technology*, edited by D. Adler, Y. Hamakawa, and A. Madan (Materials Research Society, Pittsburgh, PA, 1986), p. 3.
- ¹⁶K. K. Gleason, K. S. Wang, M. K. Chen, and J. A. Reimer, *J. Appl. Phys.* **61**, 2866 (1987).
- ¹⁷M. J. Kushner, in *Plasma Processing*, edited by J. W. Coburn, R. A. Gottscho, and D. W. Hess (Materials Research Society, Pittsburgh, PA, 1986), pp. 293-307.
- ¹⁸I. NoorBatcha, L. M. Raff, and D. L. Thompson, *J. Chem. Phys.* **81**, 3715 (1984).
- ¹⁹P. Ho, M. E. Coltrin, J. S. Binkley, and C. F. Melius, *J. Phys. Chem.* **90**, 3399 (1986).
- ²⁰D. K. Beigelsen, R. A. Street, C. C. Tsai, and J. C. Knights, *Phys. Rev. B* **20**, 4839 (1979).
- ²¹J. Shirafuji, M. Kuwagaki, T. Sato, and Y. Inuishi, *Jpn. J. Appl. Phys.* **23**, 1278 (1984).
- ²²R. Robertson, D. Hils, H. Chatham, and A. Gallagher, *Appl. Phys. Lett.* **43**, 544 (1983).
- ²³R. Robertson and A. Gallagher, *J. Appl. Phys.* **59**, 3402 (1986).
- ²⁴M. E. Coltrin, R. J. Kee, and J. A. Miller, *J. Electrochem. Soc.* **131**, 425 (1984).
- ²⁵O. Kuboi, M. Hashimoto, and Y. Yatsurugi, *Appl. Phys. Lett.* **45**, 543 (1984).
- ²⁶A. Matsuda, T. Kaga, H. Tanaka, L. Malhortra, and K. Tanaka, *Jpn. J. Appl. Phys.* **22**, L115 (1983).
- ²⁷R. A. Street, J. C. Knights, and D. K. Beigelsen, *Phys. Rev. B* **18**, 1880 (1978).